

# The Impact of High Fat Diet and Flaxseed on Liver Histology, Histochemistry and Morphometry in Ovariectomized Albino Rat

Original  
Article

*Hekmat Ahmed Sorour, Mona Abdelrahman Salem, Dina Allam Abdel Maksoud and Mona M. Abd El galil*

*Department of Histology, Faculty of Medicine for Girls, Al-Azhar University, Cairo, Egypt*

## ABSTRACT

**Background:** Postmenopausal weight gain sounds an alarm for women's health and may lead to non-alcoholic fatty liver disease. Flaxseed is rich in antioxidants and may improve liver functions. However, the precise mechanisms remain unclear.

**Objective:** This work was designed to evaluate the possible hepatoprotective role of flaxseed in ovariectomized obese female albino rat model.

**Materials and Methods:** Adult female albino rats were divided into three groups: Group I (control), Group II (High fat diet group) and Group III (bilaterally ovariectomized group) which then subdivided equally into; GIIIa (ovariectomized only group), GIIIb (ovariectomized rats fed on a high fat diet) and GIIIc (ovariectomized rats fed on high-fat diet contained ground flaxseed) till the end of the experiment. After 12 weeks, body weight, serum lipid profiles and liver enzyme levels were estimated. Liver specimens were processed for light and electron microscopic studies. Morphometric measurements and statistical analyses were done.

**Results:** Ovariectomy and high-fat diet caused a significant increase in body weight, lipid profiles and destructive changes within the liver tissue in the form of vacuolated cytoplasm, pyknotic nuclei, congested blood vessels and mononuclear inflammatory cells infiltration that was supported by a significant elevation in the liver enzymes coupled to a significant increase in the area percentage of collagen fibers and reduction in the Periodic-Acid-Schiff (PAS) reaction. The ultrastructural assessment confirmed these distortions. In contrast, flaxseed significantly corrected hyperlipidemia and hepatic biochemical parameters with critical improvement in the liver histopathological changes depicted previously.

**Conclusion:** Flaxseed may have a hepatoprotective role against steatohepatitis and fibrosis in ovariectomized obese rat model.

**Received:** 22 January 2021, **Accepted:** 18 February 2021

**Key Words:** Flaxseed, high fat diet, liver, ovariectomy, steatohepatitis.

**Corresponding Author:** Mona Mohamed Abd Elgalil, MD, Department of Histology, Faculty of Medicine (Girls), Al-Azhar University, Cairo, Egypt, **Tel.:** +20 10903 05671, **E-mail:** medicalmona2009@yahoo.com

**ISSN:** 1110-0559, Vol. 45, No.1

## INTRODUCTION

Postmenopausal obesity is sometimes the main risk factor liable for metabolic syndrome which are linked to the development of non-alcoholic fatty liver disease (NAFLD) that begins as steatosis and should progress to steatohepatitis, cirrhosis, liver failure, and hepatocellular carcinoma<sup>[1]</sup>.

Symptoms of NAFLD, if present, are vague, but ought to be suspected in patients with elevated aminotransferase levels at routine investigation. Hepatomegaly has been accounted for in up to 50% of obese subjects. Moderate and severe steatosis might be identified using ultrasonography<sup>[2]</sup>. Magnetic Resonance Image (MRI) is more sensitive techniques yet are thwarted by the cost and absence of practicality in enormous populaces<sup>[3]</sup>.

NAFLD is now and then clinically quiet without decompensate cirrhosis. Indications, if present, are vague, similar to weariness and right upper quadrant uneasiness however ought to be suspected in patients with raised aminotransferase levels at routine assessment. Most discoveries on actual assessment are likewise ordinary,

notwithstanding that, hepatomegaly has been accounted for in up to half of corpulent subjects. Radiological proof of a greasy liver utilizing ultrasonography permits recognizing moderate and extreme steatosis<sup>[2]</sup>. More delicate methods, including Magnetic Resonance Image (MRI), are blocked by the cost and absence of plausibility in huge populaces.

Liver biopsy is likely considered as the gold standard to assess the histological features of necrotic inflammation and fibrosis that define non-alcoholic steatohepatitis (NASH) and to determine its probable prognosis<sup>[4]</sup>. However, the liver biopsy has limited applicability in epidemiological and clinical studies and is not routinely performed because of the invasiveness of the procedure and its high cost<sup>[5]</sup>.

As of recently, there is no particular treatment for NAFLD that is proven to be effective. Nonetheless, a proper eating regimen and exercise program is associated with a diminishing in the incidence of metabolic syndrome and can likewise improve the histologic features of NASH in over 80% of cases<sup>[6,7]</sup>.

Medical treatment of NAFLD is the subsequent option to diminish the occurrence of metabolic syndrome, including

a lipid- bringing down medication that diminishes the content of hepatic triglyceride<sup>[8]</sup> or Insulin sensitizers<sup>[2,9]</sup>. Antioxidants can stabilize mitochondrial function, repress lipid peroxidation and resulting free radical reaction<sup>[10]</sup>.

Liver transplantation may be required if cirrhosis develops and is complicated by liver failure or hepatocellular carcinoma<sup>[11]</sup>.

In recent years, herbal medicines have been widely utilized as effective remedies for the prevention and treatment of multiple health conditions instead of using synthetic drugs as they are beneficial cost-effective natural remedies and economically available<sup>[12]</sup>.

Flaxseed or linseed (*Linum usitatissimum* L), is a well-known source of high-quality protein, soluble fiber, alpha-linolenic acid (ALA), linoleic acid essential fatty acids, several types of vitamins and minerals and phytochemicals which incorporate phenolic acids, cinnamic acids, flavonoids and lignan polyphenols that have estrogenic and anti-estrogenic hormone properties in addition to their antioxidant, anti-angiogenic, antiviral, antifungal, and anti-inflammatory non-hormonal properties that may assume a part in the anticipation and treatment of several medical issue particularly lipid disorders, coronary heart disease and may improve liver capacities<sup>[13]</sup>.

The current study aimed to assess the histological and biochemical changes in the liver of ovariectomized obese female albino rats and the effectiveness of adding crushed flaxseed to high-fat diet formula on improving these pathological changes.

## MATERIALS AND METHODS

### Animals

Thirty adult female *Rattus norvegicus* female albino rats aged 10 weeks and weighing  $145 \pm 20$  g were utilized in the current experiment. They were purchased from Helwan Breeding farm, Egypt. Rats were bred in the animal house, Faculty of Medicine for Girls, Al-Azhar University, and kept up in an air-conditioned animal house in cages at room temperature (22–25°C) with specific pathogen-free conditions, and were subjected to a 12:12-h daylight/darkness. Rats were acclimatized, one week for adaptation before the beginning of the experiment, and were allowed unlimited access to food and water throughout the experiment. All the ethical protocols for animal treatment were carried out according to the ethical procedures and guidelines of the Institutional Animal Care and Use Committee accepted by the Faculty of Medicine for Girls, Al Azhar University, Egypt.

### Diets

Diet formulas were prepared in small pellet form as set by the National Research Council (NRC) USA<sup>[14]</sup> at the Faculty of Agriculture, Al Azhar University, Cairo.

Balanced diet: The fat content in the balanced diet was about 2.3 kg fat /100 Kg diet (5.53 %) (Table 1).

**Table 1:** Balanced Diet Formula

Ingredient	Amounts in Kg / 100 K g diet
- Yellow corn	77.7 kg
- Soy bean 44 %	10.7 kg
- Corn Gluten 60 %	6.37 kg
- Di calcium phosphate	0.3 kg
- Ca carbonate	1.3 kg
- Sodium chloride	0.38 kg
- Vitamins Mix	0.3 kg
- Minerals Mix	0.1 kg
- Lecithin hydrochloride	0.55 kg
- Palm oil (rich in poly saturated fatty acids)	2.3 kg
Total amounts	100 kg
Fat %	5.53 %
Metabolizable energy	3921.86 Kcal/kg diet

High-fat diet: This diet is named "isocaloric diet" and was designed by exchanging dietary fat for carbohydrate in a crossover fashion without changing total caloric intake<sup>[15]</sup>. The fat content was increased up to 7Kg fat /100 Kg diet (10.01%) (Table 2) and was stored at 4°C.

**Table 2:** High Fat Diet Formula

Ingredient	Amounts in Kg / 100 K g diet
-Yellow corn	68 kg
- Soy bean 44 %	11.07 kg
- Corn Gluten 60 %	6.1 kg
- Wheat bran	4.9 kg
- Di calcium phosphate	0.3 kg
- Ca carbonate	1.3 kg
- Sodium chloride	0.38 kg
- Vitamins Mix	0.3 kg
- Minerals Mix	0.1 kg
- Lecithin hydrochloride	0.55 kg
- Palm oil (rich in poly saturated fatty acids)	7 kg
Total amounts	100 kg
Fat %	10.01 %
Metabolizable energy	4000 Kcal/kg diet

High-fat diet containing flaxseed: ground flaxseed was added to the high-fat diet components (Table 3) at a dose of 0.2 gm/day/rat which corresponded to the adult human dose of 50 g/day<sup>[16]</sup>.

**Table 3:** High Fat Diet Formula containing ground flaxseed

Ingredient	Amounts in Kg / 100 K g diet
-Yellow corn	67.22 kg
- Soy bean 44 %	11.1 kg
- Corn Gluten 60 %	6.1 kg
- Wheat bran	5.1 kg
- Di calcium phosphate	0.3 kg
- Ca carbonate	1.3 kg
- Sodium chloride	0.38 kg
- Vitamins Mix	0.3 kg
- Minerals Mix	0.1 kg
- Lecithin hydrochloride	0.4 kg
- Palm oil (rich in poly saturated fatty acids)	7 kg
- Ground flaxseed	0.7
Total amounts	100 kg
Fat %	10.01 %
Metabolizable energy	4000 Kcal/kg diet

### Ovariectomy

Animals were anesthetized with ether inhalation. Ovariectomies were performed according to Liu *et al.*<sup>[17]</sup>.

### Experimental design

Rats were divided into 3 groups: Group I (Control group, n=6) which was daily fed on a balanced diet. The high-fat diet group (GII) (n=6) was daily fed on a high-fat diet. Ovariectomized group (GIII) (n=18); Animals of this group were bilaterally ovariectomized and subdivided equally into; ovariectomized rats fed on a balanced diet (GIIIa), ovariectomized rats fed on a high-fat diet (GIIIb) and ovariectomized rats fed on a high-fat diet containing ground flaxseed (GIIIc) till the end of the experiment.

The treatments were proceeded for 12 weeks. Rats of all groups were weighed separately at the beginning of the experiment and at the end not long prior to collecting samples.

The percentage of weight gain (% wt) is calculated by the following equation<sup>[18]</sup>

$$\% \text{ wt} = \frac{\text{Amount of increased weight in grams}}{\text{Mean of initial weight}} \times 100$$

At the end of the experiment (12 weeks), blood was collected quickly retro-orbitally in sterile tubes utilizing a heparinized capillary tube under ether anesthesia<sup>[19]</sup> for assessment of serum total cholesterol (Tc), triglycerides (TGs), high-density lipoprotein cholesterol (HDLc) and Low-density lipoprotein cholesterol (LDLc) concentration. Hepatic enzymes (Alanine aminotransferase (ALT), Aspartate-aminotransferase (AST) were additionally determined. The assessment of lipid profiles and hepatic enzymes were measured using D-2400 and P800 analyzers (Hitachi Ltd., Tokyo, Japan) and commercially available assays using kits from Roche Diagnostics (Manheim, Germany), at AL-Azhar University Center for Virus Research and Studies (VRSC)<sup>[20]</sup>.

The right lobe of the liver samples was fixed in 10% formalin for 72 hours, processed to obtain paraffin sections of 5µm thickness and were stained with Hematoxylin and Eosin (H&E) for routine histological examination to study the general structure, Masson's trichrome stain, for staining the collagen fibers and Periodic acid Schiff's (PAS) technique for recognition of glycogen content of hepatocytes<sup>[21]</sup>.

### Electron microscopic study

Electron microscopic preparation was used to detect hepatic ultrastructure changes. Small pieces (1 mm<sup>3</sup> thickness) of liver tissue of each animal were fixed immediately in 2.5% glutaraldehyde for 24h, placed in phosphate buffer for 24 hours, post-fixed in 1% osmium tetroxide, dehydrated and embedded in resin, followed by semi-thin sections stained with toluidine blue and ultrathin sections were stained with uranyl acetate and lead citrate<sup>[22]</sup>. Sections were examined by an electron microscope JEOL, TEM 1010 (Tokyo, Japan), at the electron microscopic unit of the Regional Center for Mycology and Biotechnology (RCMB), Al Azhar University.

### Quantitative, Morphometric and Statistical Studies

Different quantitative morphometric parameters were measured in liver sections including; the area percentage of the collagen fibers in Masson's trichrome stained sections and the mean area percentage of glycogen content in hepatocytes in PAS stained sections at X100 magnification<sup>[23]</sup>. 10 non-overlapping fields from five sections of each rat in each group were chosen and analyzed morphometrically using Leica light microscope MDLSD and image analysis software at the Regional Center for Mycology and Biotechnology(RCMB), Al-Azhar University, Cairo, Egypt.

All data were statistically expressed as means ± SD and compared using the one-way analysis of variance (ANOVA) followed by Tukey's post hoc test. Level of probability (*P-value*) < 0.05 is used as the criterion of significance. Statistical analysis was performed using the Statistical Package for the Social Sciences, Version 22 for Windows (California, USA)<sup>[24]</sup>.

## RESULTS

### Histological results

#### Hematoxylin and Eosin (H&E) stain (Figures1a-1j)

H&E stained sections from the control group (GI) revealed the normal histological architecture of liver parenchyma comprised of branching and anastomosing cords of hepatocytes radiating from the central vein and separated from each other by hepatic blood sinusoids that appeared as narrow elongated gaps radiating from the center to periphery of the lobule and were lined by flat endothelial cells. At the corners of the lobules, portal tracts contained branches of the hepatic artery, portal vein and bile ducts could be seen (Figure 1a). The polygonal

hepatocytes had eosinophilic cytoplasm and centrally located rounded vesicular nuclei with prominent nucleoli. Some cells appeared binucleated (Figure 1b).

H&E stained sections from the high-fat diet group (GII) showed enlarged hepatocytes had multiple intracytoplasmic vacuoles of different sizes with shrunk, irregular and darkly stained nuclei surrounding dilated central vein and dilated congested branches of the hepatic portal vein. Some normal hepatocytes were also observed (Figures 1c,1d). Mononuclear inflammatory cell infiltration close to the portal tract area was also detected as compared to that of the control group (Figure 1d).

Inversely, examination of the H&E stained liver sections of the ovariectomized rats fed on a balanced diet (GIIIa) revealed regular orientation of the hepatocyte plates. Some vacuolated hepatocytes with pyknotic nuclei were seen surrounding dilated central vein and near the portal tract area. However, the remaining hepatocytes were nearly normal (Figures 1e,1f). Mononuclear cell infiltration was also observed (Figure 1f).

H&E stained sections from the ovariectomized rats fed on the high-fat diet (GIIIb) showed irregular orientation of the hepatocyte plates, congested central vein as well as dilated congested branches of the hepatic portal vein (Figures 1g,1h). Enlarged hepatocytes appeared irregular in shape with widespread random distribution of large intracytoplasmic vacuoles with a peripheral displacement of the nucleus. Some vacuoles coalesced with each other. Others had multiple intracytoplasmic vacuoles. Hemorrhagic areas along with widespread inflammatory cell infiltration were noticed in between the hepatocytes and close to the congested blood vessels (Figure 1h).

While H&E examination of liver sections of the ovariectomized rats fed on a high-fat diet contained crushed flaxseed (GIIIc) showed that the structure of the liver was comparable to that of the control group. Few vacuolated hepatocytes with minimal cellular infiltration were mainly observed near the portal tract area (Figures 1i,1j).

#### **Masson's trichrome stain (Figures 2a-2f)**

Liver sections stained with Masson's trichrome stain revealed fine collagen fibers surrounding the central vein and portal area in the control group (GI) (Figure 2a).

While in the high-fat diet group (GII) apparent increase in the density and distribution of collagen fibers was noticed around the central vein, the portal area and areas connecting the central vein and portal tracts (Figure 2b).

In ovariectomized rats fed on a balanced diet (GIIIa), there was an increase in the density of collagenous fibers at the portal tract area (Figure 2c).

The ovariectomized rats fed on the high-fat diet (GIIIb) showed increased collagen fibers distribution within at the portal tract area compared with the control group (Figure 2d) with the appearance of collagen fibers invested between highly vacuolated hepatocytes in a pattern referred to as "chicken wire" fibrosis (Figure 2e).

Inversely, ovariectomized rats fed on a high-fat diet contained crushed flaxseed group (GIIIc) showed that the collagenous fibers distribution was quite similar to the control (Figure 2f).

#### **Periodic acid Schiff technique (Figures 3a-3f)**

PAS stained sections of the control group (GI) showed strong PAS +ve glycogen granules occupying most of the cytoplasm of the hepatocytes at the pericentral and portal areas of the hepatic lobules (Figure 3a).

While in the high-fat diet group (GII) there was a reduction in the PAS-positive or even negative reaction in the vacuolated hepatocytes compared with the control group opposite to those hepatocytes in the remaining areas of hepatic lobules showed strong reaction (Figure 3b).

In the ovariectomized rats fed on a balanced diet (GIIIa), the PAS reaction was closely similar to that of the control group (Figure 3c).

While ovariectomized rats fed on a high-fat diet (GIIIb) revealed widespread negative and weak PAS reaction within the pericentral (Figure 3d) and periportal areas of hepatic lobules (Figure 3e).

Inversely, ovariectomized rats fed on a high-fat diet contained crushed flaxseed (GIIIc) revealed a nearly normal distribution of glycogen granules in the parenchymal liver cells that was almost similar to that of the control group (Figure 3f).

#### **Ultrastructural examination**

Transmission electron microscopic (TEM) liver sections from the control group (GI) revealed normal hepatocytes which were polygonal in shape, had central rounded euchromatic nuclei and well-defined nucleoli. The blood sinusoids were lined by a discontinuous sheet of endothelial cells. The perisinusoidal space was studded with microvilli (Figure 4a). The cytoplasm of the hepatocytes contained well-developed rough endoplasmic reticulum, interconnected channels of the smooth endoplasmic reticulum as well as multiple ovoid, rounded or rod-like mitochondria with intact cristae (Figure 4b). Clusters of glycogen granules were seen in the cytoplasm of the hepatocytes (Figure 4d). Bile canaliculi were studded with microvilli and the canalicular lumen was sealed by the tight junction between adjacent hepatocytes (Figure 4b). The processes of Kupffer cells were observed spanned the sinusoidal lumen and intermingled with microvilli of the hepatocytes. Kupffer cell nuclei had peripherally arranged heterochromatin (Figure 4c). Besides, ITO cell (hepatic stellate cell) was observed in the perisinusoidal region as a cell with irregular outlines that were surrounded by the microvilli of hepatocytes. The cytoplasm of hepatic stellate cell contained homogenous electron lucent lipid droplets of variable sizes. The nucleus was occasionally indented or compressed by lipid droplets (Figure 4d).

The most apparent finding in the high-fat diet group (GII) was an accumulation of numerous variable-

sized electron lucent lipid droplets coalesced with each other throughout the cytoplasm of hepatocytes (Figure 5a) as well as abnormal giant expanded and swollen mitochondria of irregular forms and size near some dilated rough endoplasmic reticulum and clusters of glycogen granules (Figure 5b). Scattered heterogenous lysosomes and multivesicular bodies could be also detected (Figure 5c). The cytoplasm of the Kupffer cell had a large indented nucleus as well as lysosomes and phagocytic vesicles. Collagen bundles cut in different directions were also observed (Figure 5d).

There were no obvious changes in hepatocytes cytoplasm of the ovariectomized rats fed on a balanced diet (GIIIa) except a few variable-sized electron lucent lipid droplets (Figures 6a-6d), normal mitochondria as well as normal rough endoplasmic reticulum and glycogen granules were observed scattered within the cytoplasm of the hepatocytes (Figures 6b,6c). Kupffer cell in the blood sinusoid showed normal appearance more or less as the control group (Figure 6d).

In contrast, ovariectomized rats fed on a high-fat diet (GIIIb) revealed numerous large sized electron lucent lipid droplets coalesced with each other almost filled the cytoplasm of hepatocytes (Figures 7a,7d). Hepatic blood sinusoids contained many inflammatory cells, mostly lymphocytes (Figure 7a). Multiple degenerated irregular giant mitochondria in proximity with abundant markedly dilated rough endoplasmic reticulum and heterogeneous secondary lysosomes appeared separated by large areas of rarified cytoplasm (Figure 7b). Nuclear margination as well as condensed opaque matrices of mitochondria without any internal organization with a few arrays of broken rough endoplasmic reticulum were seen within the rarified cytoplasm (Figure 7c). Lipid droplets were observed inside the blood sinusoid and in the cytoplasm of the endothelial cell with apoptotic irregular nuclei that showed chromatin condensation (Figure 7d). Kupffer cell with large indented nucleus, lysosomes and phagocytic vesicles could be detected (Figure 7e). Myofibroblast cell appeared flat with well developed dilated rough endoplasmic reticulum, increased spacing within the nuclear envelop and few lipid droplets. Cross-sections of collagen bundles nearby flattened myofibroblast cell were also observed (Figure 7f).

Sections of the treated group with crushed flaxseed (GIIIc) showed nearly normal ultrastructure of the hepatocytes that appeared more or less as the control group (Figures 8a-8d).

### **Statistical results**

#### **Body weight**

The mean values of initial body weight (IBW) of all studied groups were nearly similar with no statistically significant difference. They ranged from  $145.4 \pm 5.5$  to  $150 \pm 8.6$

At the end of the experiment, a significant increase in the mean final body weight (FBW) in the high-fat diet

group (GII) and the ovariectomized rats fed on high-fat diet (GIIIb) that showed the highest percentage of weight gain (%) when compared to the other experimental groups. While the least recorded mean of FBW was among the ovariectomized rats fed on a high-fat diet that contained crushed flaxseed (GIIIc) followed by ovariectomized rats fed on the balanced diet (GIIIa) with a statistically significant difference ( $P < 0.05$ ). However, the reduction in the FBW and the % of weight gain in GIIIa and GIIIc could not reach the control values as there were significant differences when compared to the control group ( $P < 0.05$ ) (Table 4, Histogram 1).

### **Biochemical results**

#### **Effect on serum lipid profile**

At the end of the experiment, serum analyses for lipid profile assay among rats of all experimental groups were illustrated in (Table 5, Histogram 2). The highest recorded mean values of TC, TG and LDLc levels were among the ovariectomized rats fed on a high-fat diet (GIIIb) and the high-fat diet group (II) respectively coupled with a significant decrease in HDLc level when compared to the other experimental groups ( $P < 0.05$ ).

Inversely, the least recorded mean of TC, TG and LDLc levels were among the ovariectomized rats fed on high-fat diet contained crushed flaxseed (GIIIc) followed by ovariectomized rats fed on a balanced diet (GIIIa) respectively coupled with a significant increase in HDLc level when compared to the high-fat diet groups (GII & GIIIb) ( $P < 0.05$ ) and a non-significant values when compared with the control group (I) ( $p > 0.05$ ) except for TC & LDLc levels ( $P < 0.05$ ).

#### **Effect on serum liver enzymes**

The statistical study concerning serum liver enzymes; AST and ALT among rats of all experimental groups revealed that the highest mean values were recorded among the ovariectomized rats fed on a high-fat diet (GIIIb) and the high-fat diet group (II) respectively when compared to the other experimental groups ( $P < 0.05$ ).

Interestingly, ground flaxseed in group IIIc improved all these parameters as demonstrated by a significant decrease in AST and ALT when compared to the high-fat diet groups (GII & GIIIb) ( $P < 0.05$ ). The best-recorded data was among GIIIa. However, improvement in all measured parameters could not reach the control values as there was a significant difference when compared to the control group ( $P < 0.05$ ) (Table 6, Histogram 3).

### **Histomorphometric results**

#### **Area percent of collagen**

Using Masson's trichrome stained sections, there was a significant increase in the mean area percentage of collagen fibers in the high-fat diet group (GII) and the ovariectomized rats fed on a high-fat diet (GIIIb) that showed the highest percentage when compared to the other

experimental groups. Inversely, the least recorded mean of collagen was among the ovariectomized rats fed on a high-fat diet contained crushed flaxseed (GIIIc) followed by ovariectomized rats fed on a balanced diet (GIIIa) respectively when compared to the high-fat diet groups (GII & GIIIb) ( $P<0.05$ ). However, the reduction in area % of collagen could not reach the control values as there was a significant difference when compared to the control group ( $P<0.05$ ) (Table 7, Histogram 4).

#### Area percent of glycogen content in PAS stained section

The area % of glycogen content in PAS stained sections

of the ovariectomized rats fed on a high-fat diet (GIIIb) showed the least mean when compared to the other experimental groups. Inversely, the ovariectomized rats fed on a high-fat diet contained crushed flaxseed (GIIIc) showed a significant increase in area % of glycogen content when compared with the high-fat diet groups (GII & GIIIb) ( $P<0.05$ ) despite that, the increase in area % of glycogen could not reach to the control values as there was a significant difference when compared to the control group ( $P<0.05$ ) (Table 7, Histogram 5).

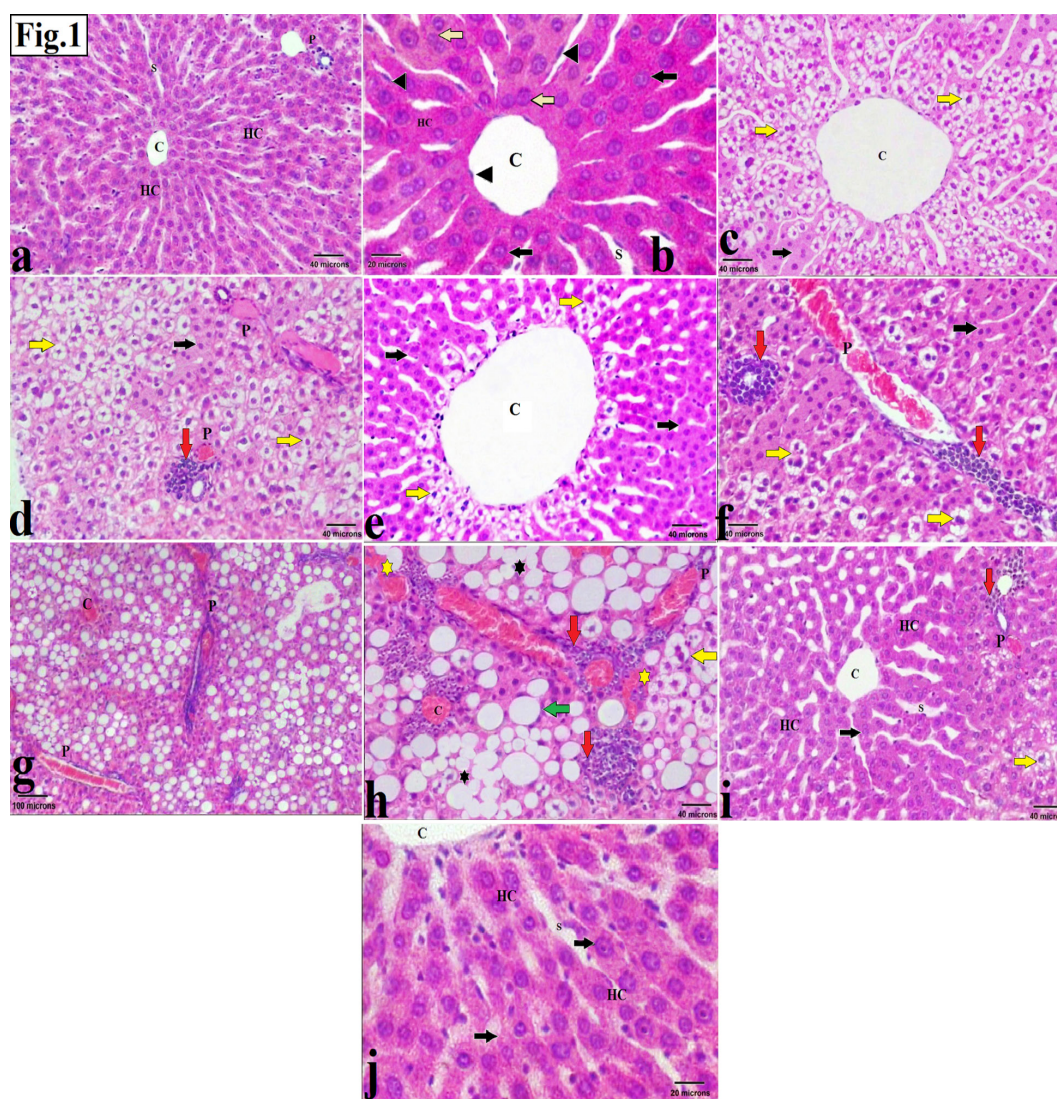


**Fig. 1:** Photomicrographs of the liver tissue from the experimental groups: control (a-b) showing: anastomosing hepatic cords (HC), the central vein (C) and blood sinusoids (S). Notice, portal tract (P) at the corner of the hepatic lobule. (b) polyhedral hepatocytes with eosinophilic cytoplasm, central rounded and vesicular nuclei (black arrow). Some cells appear binucleated (white arrows). Blood sinusoids (S) and central vein (C) are lined by flat endothelial cells (arrowheads). High-fat diet group (c-d) show: widespread vacuolated hepatocytes with central rounded darkly stained nuclei (yellow arrows). Normal hepatocytes (black arrows) appear near dilated central vein (C) and congested portal veins (P). Notice, mononuclear cell infiltration (red arrow) close to the portal tract area. Ovariectomized only group (e-f), demonstrating: regular orientation of the hepatocyte plates, few vacuolated hepatocytes (yellow arrows) around the dilated central vein (C) and congested portal vein (P). Normal hepatocytes (black arrows) and inflammatory cell infiltration (red arrows) are noticed. Ovariectomized rats fed on high-fat diet (g-h) show: distortion of the hepatic plates, congestion of central vein (C), hepatic portal veins (P) and widespread vacuolated hepatocytes with peripherally located nuclei (green arrow). Some vacuoles coalesce with each other (black stars). Other hepatocytes have multiple intracytoplasmic vacuoles (yellow arrow). Extensive inflammatory infiltration (red arrows) and hemorrhagic areas (yellow stars) are also seen. Ovariectomized rats fed on a high-fat diet contained crushed flaxseeds (i-j) show: normal anastomosing hepatic cords (HC), central vein (C) and blood sinusoids (S). Most hepatocytes appear normal (black arrows). Few focal areas of vacuolated hepatocytes (yellow arrow) and inflammatory cell infiltration (red arrow) are seen near the portal tract area. [H&E; (a, c-f, h-i) X100, Scale bar; 40µm, (b,j) X200, Scale bar; 20µm & (g) X40, Scale bar; 100µm]

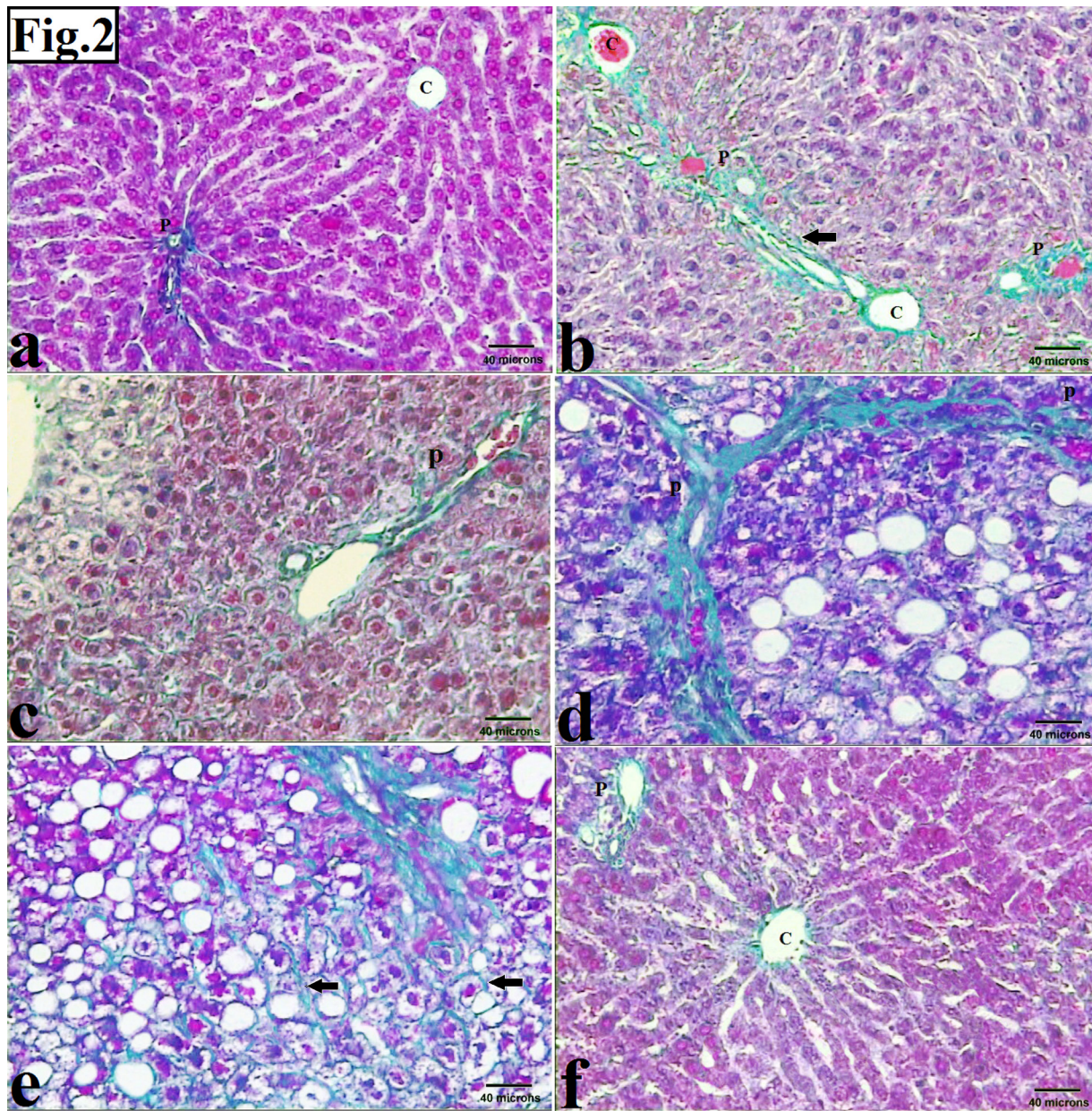


**Fig. 2:** Photomicrographs of the liver tissue from the experimental groups; GI (a) showing: Normal distribution of fine collagen fibers around the central vein (C) and portal tract area (P). GII (b) shows; increase in the density of collagen fibers around central veins (C), portal tracts (p) and areas connecting them (arrows). GIIIa (c), demonstrating: slight increase in the collagen fibers at portal tract area (p). GIIIb (d-e) show: marked increase in the collagenous fibers distribution at the portal tract area (P) as well as "chicken wire" appearance (arrows). GIIIc (f) show: normal distribution of fine collagen fibers around the central vein (C) and portal tract area (P). [Masson's trichrome X 100 , Scale bar; 40µm].

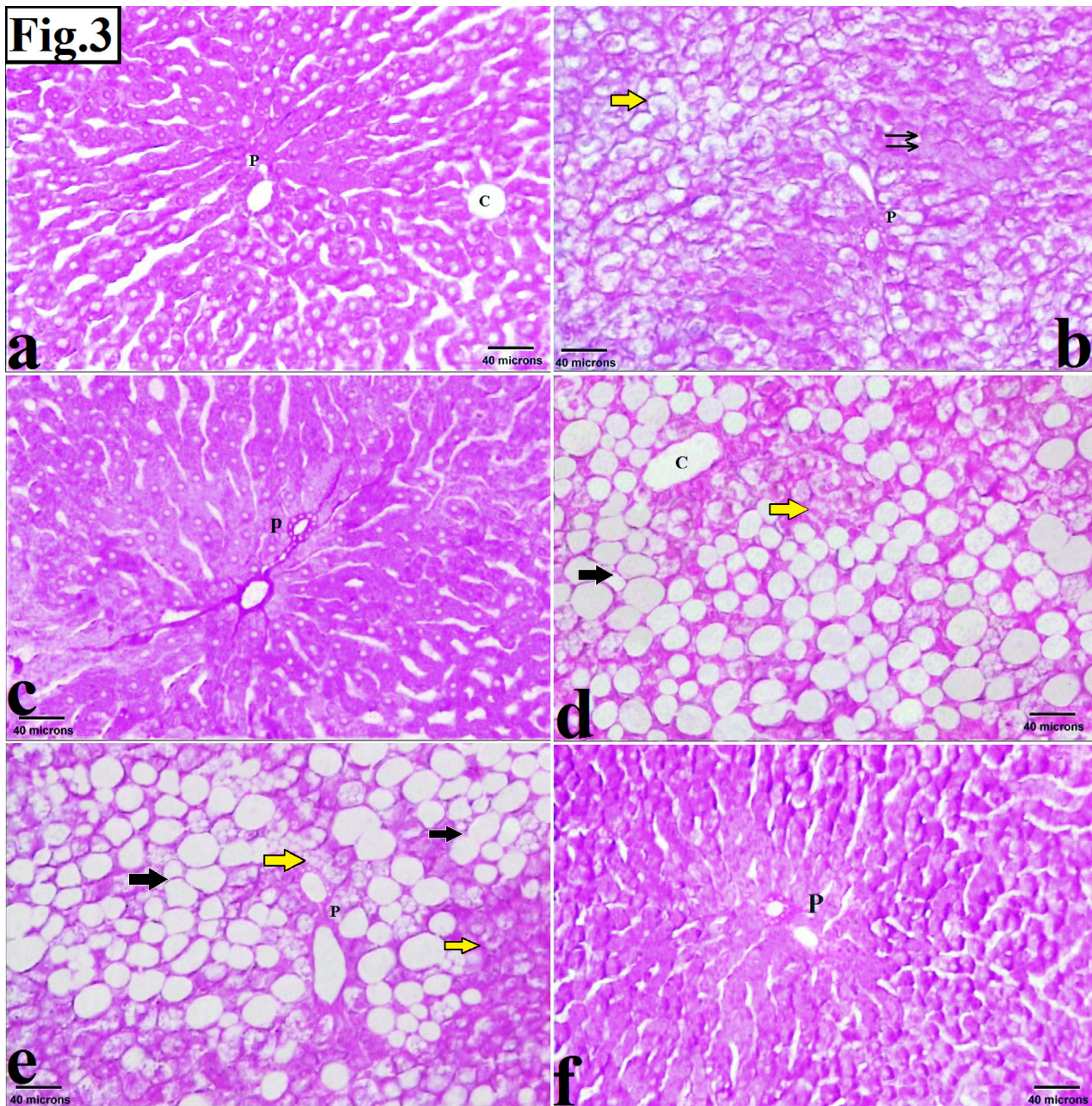


**Fig. 3:** Photomicrographs of the liver tissue from the experimental groups: GI (a) showing: strong PAS reaction within most of hepatocytes cytoplasm surrounding the central vein (C) and portal area (P). GII (b), shows a widespread reduction of PAS reaction in vacuolated hepatocytes (yellow arrow) and strong reaction in the remaining hepatocytes (double arrow) near the portal area (P). GIIIa (c), demonstrating: high restoration of the PAS + ve reaction in most hepatocytes and surrounding portal area (P). GIIIb (d-e) show: widespread negative PAS reaction (black arrows) and areas of weak PAS reaction (yellow arrows) in some hepatocytes within the pericentral (C) and periportal areas (p) of hepatic lobules. GIIIc (f) show: strong PAS reaction within most of hepatocytes and near the portal area (P). [PAS reaction x 100, Scale bar; 40 $\mu$ m]



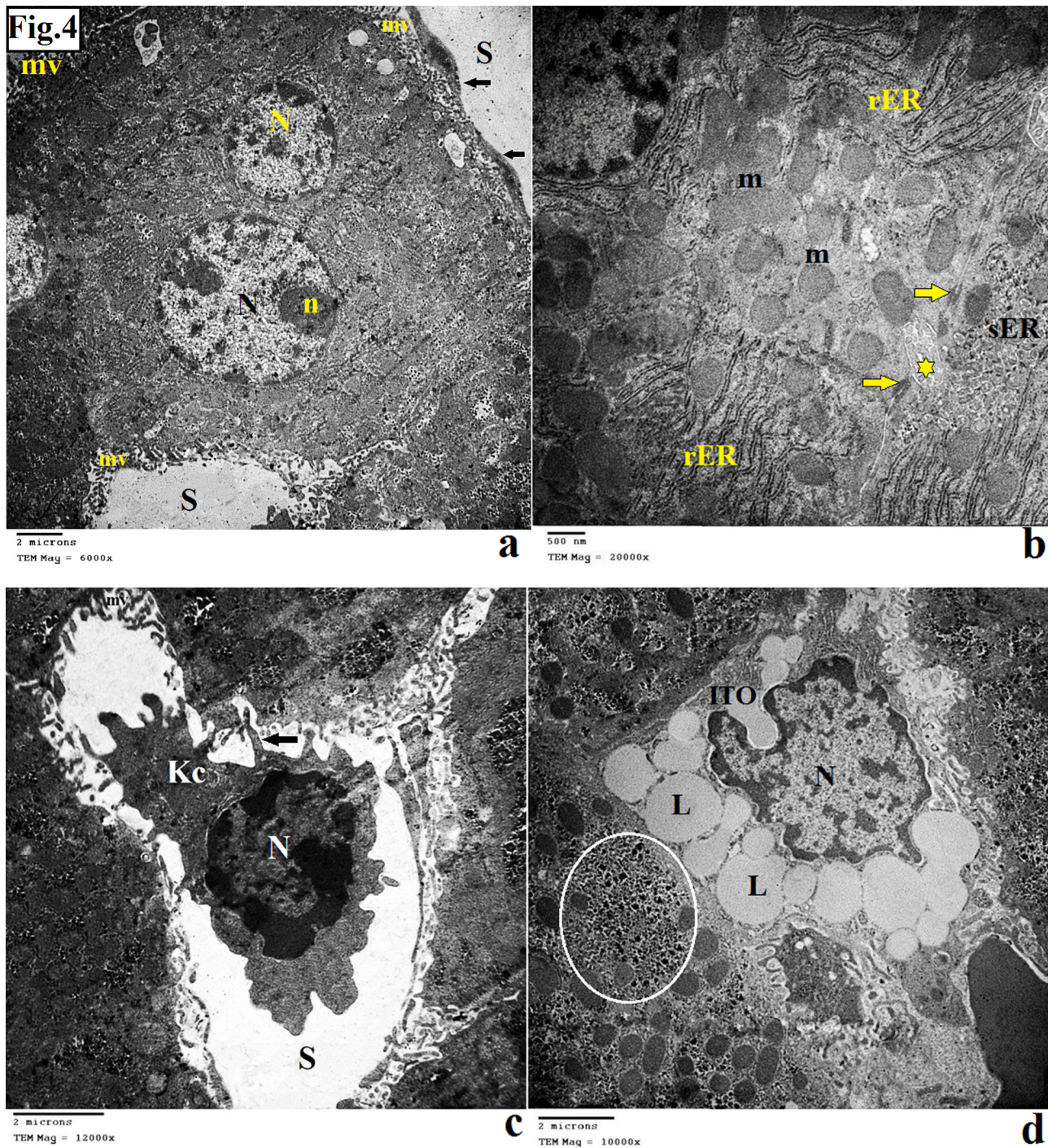


**Fig. 4:** TEMs of liver sections from GI showing: (a) Binucleated hepatocyte has euchromatic nuclei (N) and prominent nucleoli (n). Notice, numerous microvilli (mv) occupy the perisinusoidal space and hepatic blood sinusoids (S) is lined by endothelial cells (arrows). (b) Flattened cisternae of the rough endoplasmic reticulum (rER), many mitochondria (m) of variable shape and size and smooth endoplasmic reticulum (sER) near bile canaliculi (yellow star). Notice, microvilli in the lumen of the bile canaliculi (yellow star) with desmosomal junctions (yellow arrows) connecting the adjacent hepatocytes. (c) Kupfer cell (Kc) in hepatic sinusoid (S) has a large heterochromatic nucleus (N) with characteristic pseudopodia intermingle with microvilli of hepatocytes (arrow). (d) The cytoplasm of the hepatic stellate cell (ITO) has homogenous lipid droplets (L) and occasionally indented nucleus (N). Clusters of glycogen granules (circle) are seen in the cytoplasm of the adjacent hepatocyte. [a, X6000; b, X20000; c, X12000 & d, X10000]

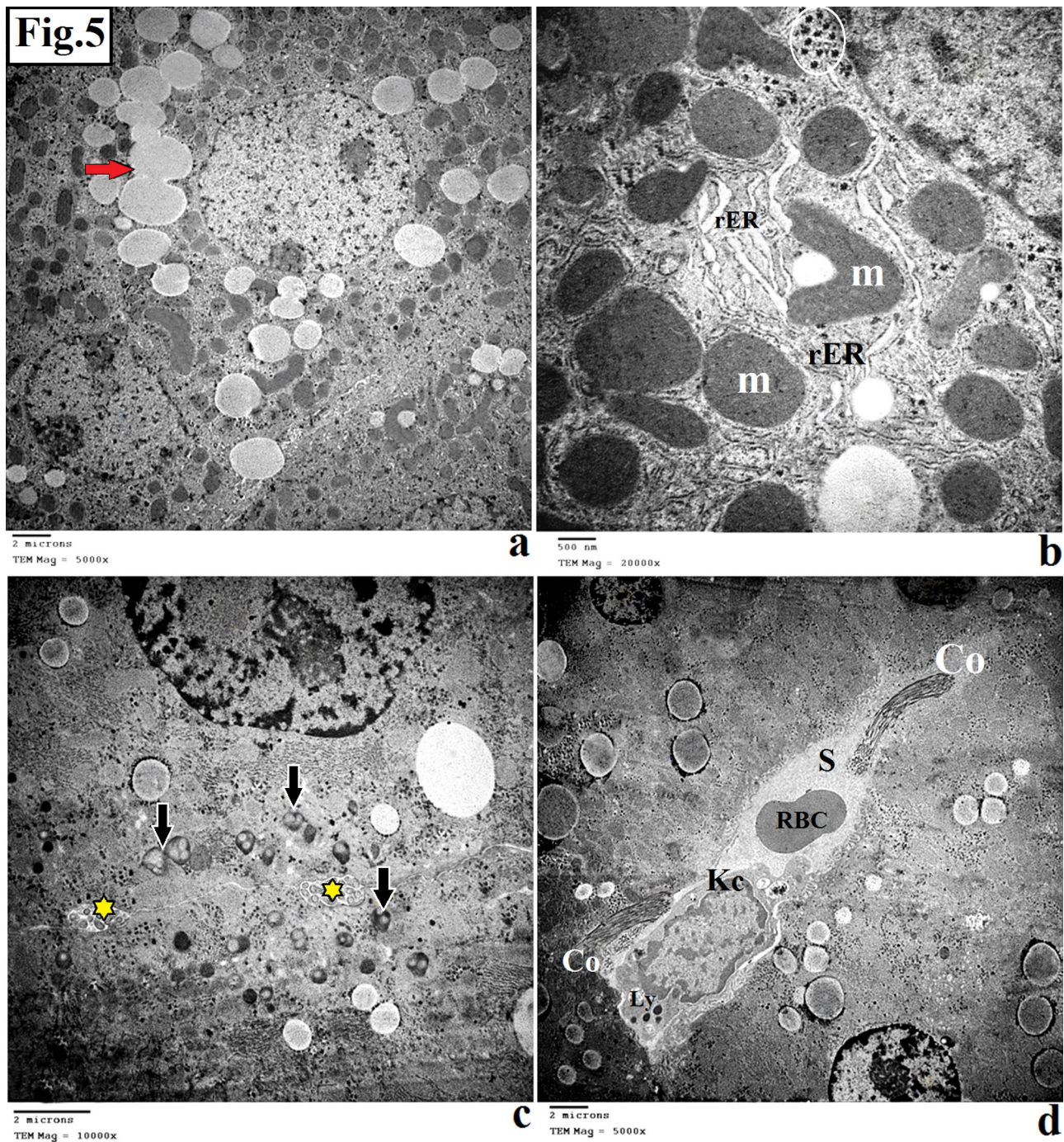


**Fig. 5:** TEMs of liver sections of animals from GII showing: (a) Numerous lipid droplets (L) coalesce with each other throughout the cytoplasm of the hepatocytes (red arrow), (b) Some dilatation of rough endoplasmic reticulum (rER) envelope abnormal giant mitochondria (m). Clusters of glycogen granules (circle) are also observed. (c) Heterogenous secondary lysosomes (arrows) and lipid droplets (L) within the hepatocyte cytoplasm. Bile canaliculi (yellow stars) appear between adjacent hepatocytes with microvilli in its lumen. (d) Blood sinusoid (S) contains red blood corpuscles (RBC) and Kupffer cell (Kc) with a large indented nucleus, lysosomes (Ly) and phagocytic vesicles in its cytoplasm as well as collagen bundles (Co) cut in different directions. [a, X5000; b, X20000; c, X10000 & d, X5000]

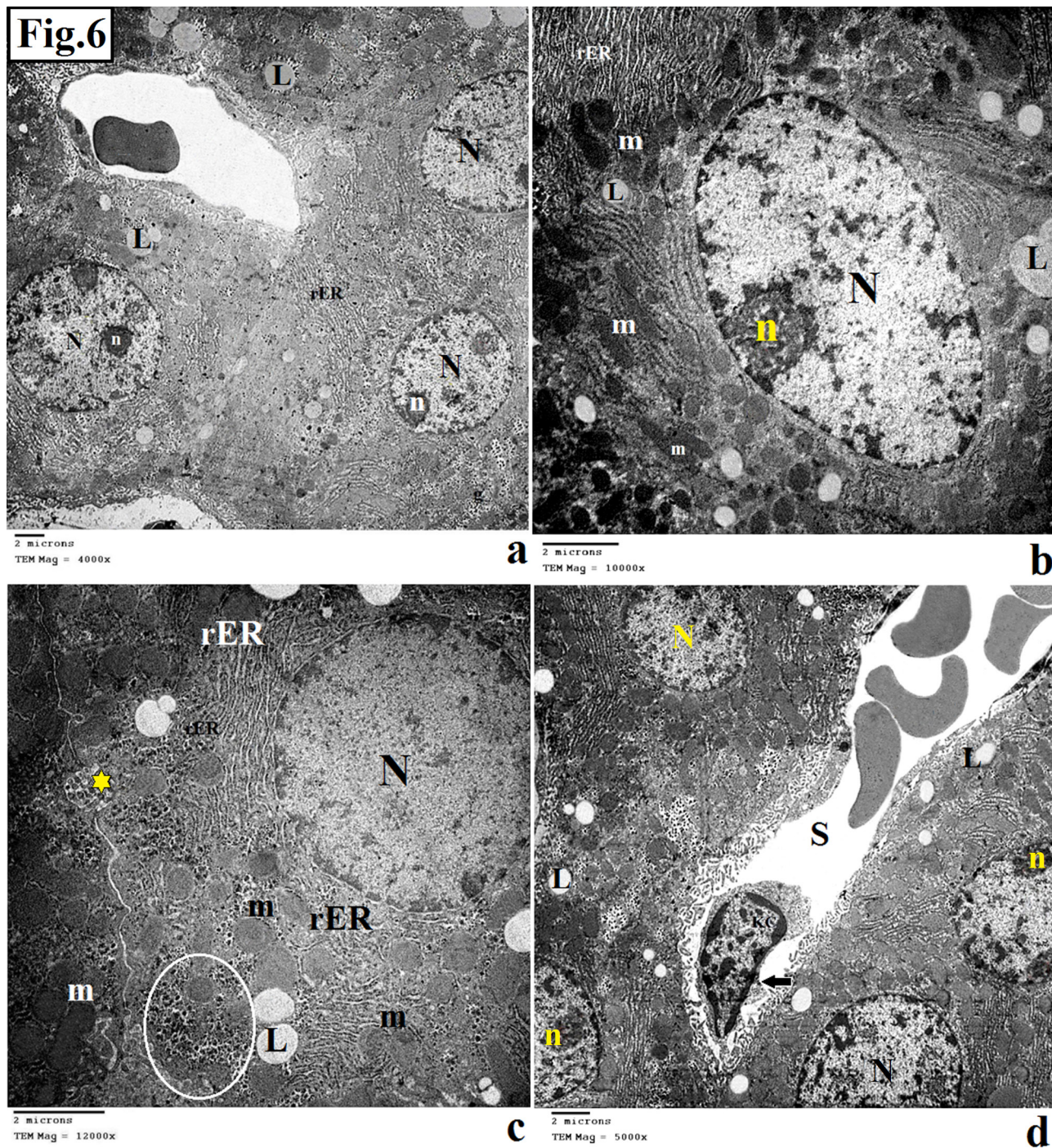


**Fig. 6:** TEMs of liver sections from Gilla showing: (a-d) Hepatocytes have euchromatic nuclei (N) and prominent nucleoli (n), few variable-sized lipid droplets (L), normal mitochondria (m) and rough endoplasmic reticulum (rER) throughout the cytoplasm of the hepatocytes. (c) Clusters of glycogen granules (circle) within hepatocyte cytoplasm. Notice, bile canaliculi (yellow star) with microvilli in its lumen. (d) Kupffer cell (Kc) in blood sinusoid (S) has a large indented nucleus and a characteristic pseudopodia (arrow) [a, X4000; b, X10000; c, X12000 & d, X5000]

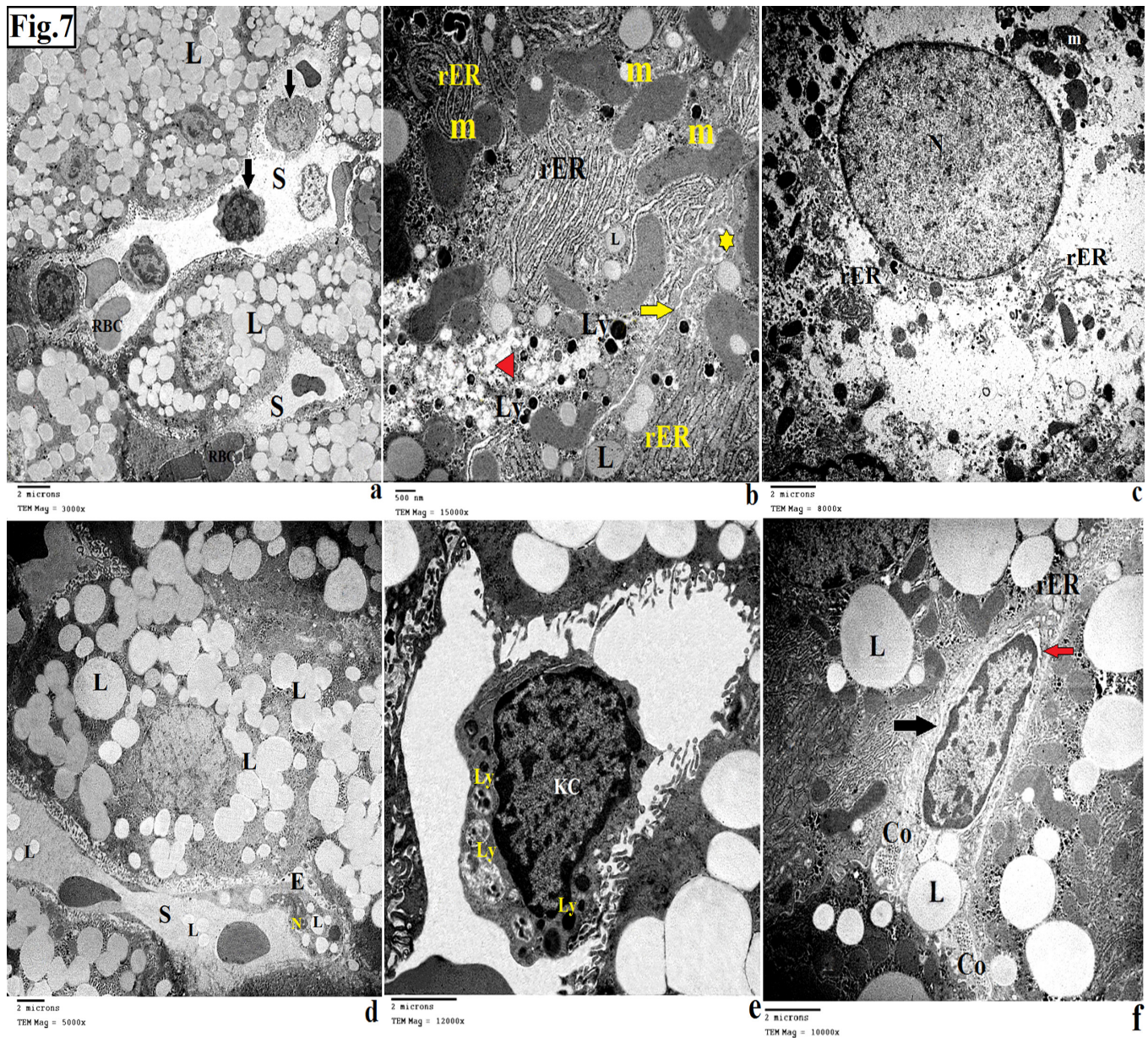


**Fig. 7:** TEMs of liver sections from GIIIB showing: (a) Numerous lipid droplets (L) filling most of the cytoplasm of the hepatocytes and coalesce with each other. Notice, blood sinusoids (S) in between hepatocytes contain red blood corpuscles (RBC) and multiple lymphocytes (black arrows). (b) Abnormal irregular swollen mitochondria (m), dilated rough endoplasmic reticulum (rER), abundant secondary lysosomes (Ly), lipid droplets (L) as well as areas of rarified cytoplasm (arrowhead) throughout the cytoplasm of the hepatocytes. Notice, microvilli in the lumen of the bile canaliculi (yellow star) with desmosomal junctions (yellow arrows) connecting the adjacent hepatocytes. (c) Electron-dense clusters of mitochondria (m) with the broken rough endoplasmic reticulum (rER) and nuclear margination (N) in the cytoplasm of the degenerated hepatocytes. (d) Lipid droplets (L) occupy most of the hepatocyte cytoplasm and appear in blood sinusoid (S) and sinusoidal endothelial cells (E) with condensed pyknotic nucleus (N). (e) Kupffer cell (Kc) has large indented nucleus, lysosomes (Ly) and phagocytic vesicles. (f) A flat myofibroblast (black arrow) shows dilated rough endoplasmic reticulum (rER) and few lipid droplets (L) in its cytoplasm with the increased spacing within the nuclear envelope (red arrow). Notice, cross-sections of collagen bundles (Co) near the flattened myofibroblast [a, X3000; b, X15000; c, X8000; d, X5000; e, X12000 & f, X10000]

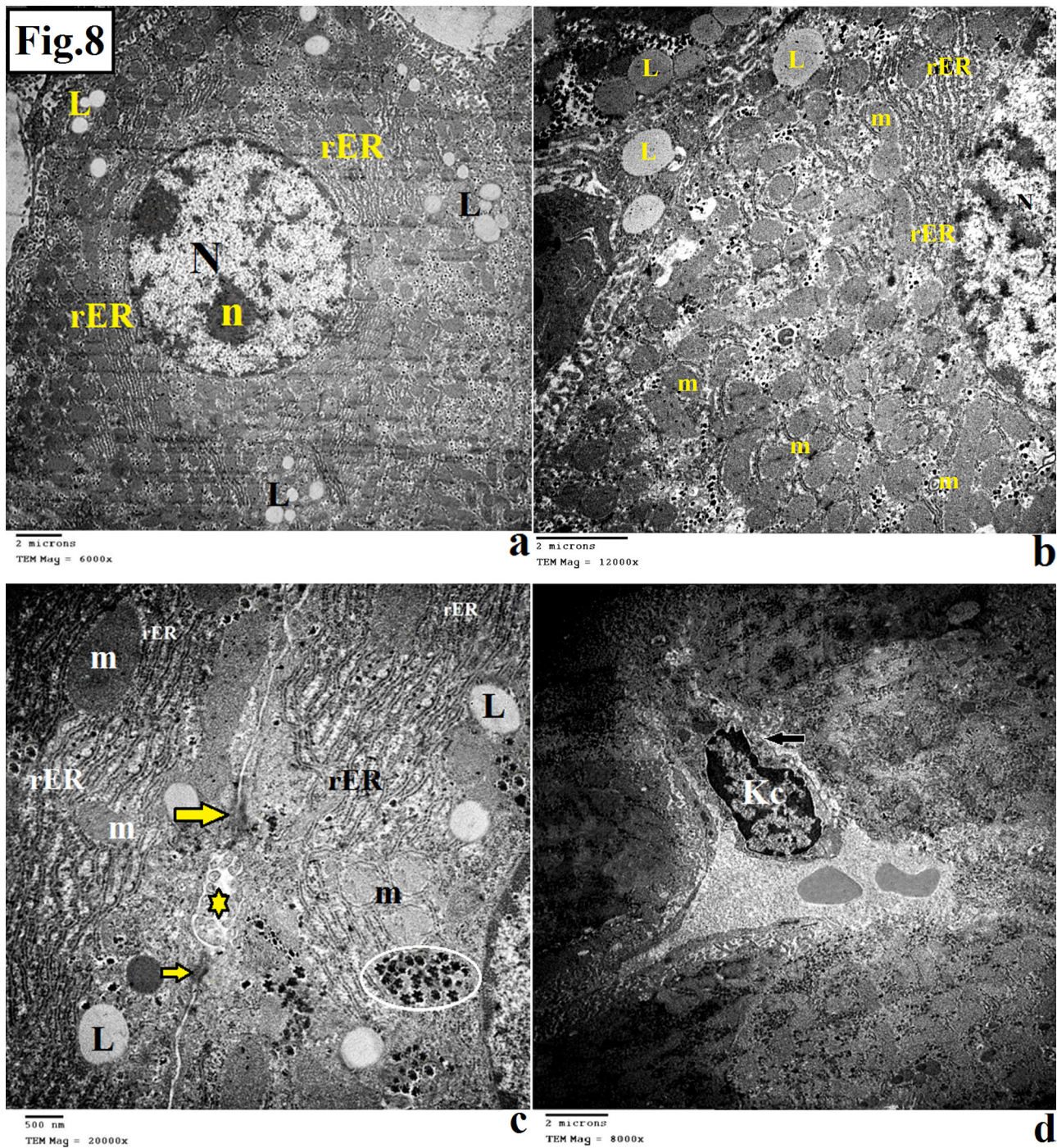


**Fig. 8:** TEMs of liver sections from GIIc showing: (a-c) Few variable-sized lipid droplets (L), flattened cisternae of the rough endoplasmic reticulum ( rER) and normal mitochondria (m) throughout the hepatocytes cytoplasm. (a) Euchromatic nucleus (N) with prominent two nucleoli (n). (c) Bile canaliculi (yellow star) appear with microvilli in its lumen. Notice, clusters of glycogen granules (circle) throughout hepatocyte cytoplasm. (d) Kupffer cell (Kc) has a large indented nucleus and a characteristic pseudopodia (arrow) intermingle with microvilli of hepatocytes [a, X6000; b, X12000; c, X20000 & d, X8000]

**Table 4:** The mean values of initial and final body weight (g) and percentage of weight gain (%) among all the experimental groups.

parameters	Groups					Test of significance	P
	Group (I) N = 6	Group (II) N = 6	Group (IIIa) N = 6	Group (IIIb) N = 6	Group (IIIc) N = 6		
Initial body weight (g)	145±5.5	150±8.6	150±6.3	148.3±4.1	145±3.2	ANOVA F=1.5	0.2
Final body weight (g)	189.2±14	240±10 <sup>■</sup>	228.3±12 <sup>▲°</sup>	247.5±5.2 <sup>■</sup>	220±11 <sup>▲°</sup>	ANOVA F=55	0.000*
Percentage of weight gain (%)	30.5± 2.3	60±2.6 <sup>■</sup>	52.2±5.3 <sup>▲°</sup>	66.9± 5.9 <sup>■</sup>	52±3.8 <sup>▲°</sup>	ANOVA F=354	0.000*

Data are presented as means ± standard deviation (SD)

N = Number of animals , g = grams

\* =  $P \leq 0.05$  = Significant

$P > 0.05$  = Non significant

■ A significant increase compared with all other groups.

▲ A significant decrease compared with high fat diet group (GII) and ovariectomized rats fed on high fat diet (GIIIb)

° A significant increase compared with control group (GI).

**Table 5:** The mean values of serum lipid profile levels (mg/dl) among the experimental groups at the end of 12<sup>th</sup> week.

parameters	Groups					Test of significance	P
	Group (I) N = 6	Group (II) N = 6	Group (IIIa) N = 6	Group (IIIb) N = 6	Group (IIIc) N = 6		
TC	48.1±2.2	76.5±4 <sup>■</sup>	53.5±2 <sup>▲°</sup>	92±7.5 <sup>■</sup>	52 ±3 <sup>▲°</sup>	ANOVA F=130	0.000*
TG	31.2±6	93.2±6.2 <sup>■</sup>	42.1±2.5 <sup>▲°</sup>	103±10 <sup>■</sup>	34±7.3 <sup>▲</sup>	ANOVA F=163	0.000*
LDLc	2.9±1.6	33.6±2 <sup>■</sup>	13±1.2 <sup>▲°</sup>	48±5 <sup>■</sup>	6.3±2.2 <sup>▲°</sup>	ANOVA F=52.4	0.000*
HDLc	39±2.2	25±2 <sup>°</sup>	35±2 <sup>▲</sup>	22±3 <sup>°</sup>	38.5±4 <sup>▲</sup>	ANOVA F=341	0.000*

Data are presented as means ± standard deviation (SD)

N = Number of animals; TC= Total Cholesterol; TG = Triglyceride; LDLc = Low density lipoprotein cholesterol & HDLc= High density lipoprotein cholesterol

\* =  $P \leq 0.05$  = Significant

■ A significant increase compared with all other groups.

° A significant decrease compared with all other groups.

▲ A significant decrease compared with high fat diet group (GII) and ovariectomized rats fed on high fat diet (GIIIb)

▲ A significant increase compared with high fat diet group (GII) and ovariectomized rats fed on high fat diet (GIIIb)

° A significant increase compared with control group (GI).

**Table 6:** The mean values of serum hepatic enzymes levels (U/l) among all the experimental groups at the end of 12<sup>th</sup> week.

parameters	Groups					Test of significance	P
	Group (I) N = 6	Group (II) N = 6	Group (IIIa) N = 6	Group (IIIb) N = 6	Group (IIIc) N = 6		
AST	35.4±6.4	49.2±7.3 <sup>■</sup>	40.5±11 <sup>▲°</sup>	53.4±11 <sup>■</sup>	42±18 <sup>▲°</sup>	ANOVA F=1.9	0.000*
ALT	23.1±2.5	52±9 <sup>■</sup>	31±3 <sup>▲°</sup>	55.6±7 <sup>■</sup>	36.3±15 <sup>▲°</sup>	ANOVA F=16	0.000*

Data are presented as means ± standard deviation (SD)

N = Number of animals; AST= Aspartate Transaminase; ALT= Alanine Transaminase

\* =  $P \leq 0.05$  = Significant

■ A significant increase compared with all other groups.

▲ A significant decrease compared with high fat diet group (GII) and ovariectomized rats fed on high fat diet (GIIIb)

° A significant increase compared with control group (GI).

**Table 7:** The mean values of area % of collagen and area % of glycogen content among all the experimental groups.

parameters	Groups					Test of significance	P
	Group (I) N = 6	Group (II) N = 6	Group (IIIa) N = 6	Group (IIIb) N = 6	Group (IIIc) N = 6		
Area % of collagen	2.9±0.5	12.9±1.4 <sup>▲</sup>	4.5±0.9 <sup>▲◊</sup>	25.7±1.2 <sup>▲</sup>	5.9±0.6 <sup>▲◊</sup>	ANOVA F=529	0.000*
Area % of glycogen	57.3.1±4.2	39.7±2.1 <sup>◊</sup>	46±2.8 <sup>▲</sup>	28.3±2.3 <sup>◊</sup>	51.2±2.1 <sup>▲</sup>	ANOVA F=96	0.000*

Data are presented as means ± standard deviation (SD)

N = Number of animals

\* = P ≤ 0.05 = Significant

■ A significant increase compared with all other groups.

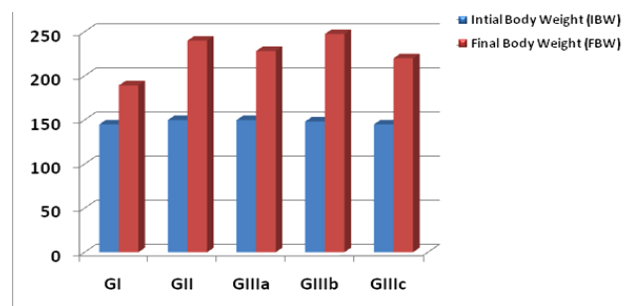
◊ A significant decrease compared with all other groups.

▲ A significant decrease compared with high fat diet group (GII) and ovariectomized rats fed on high fat diet (GIIIb)

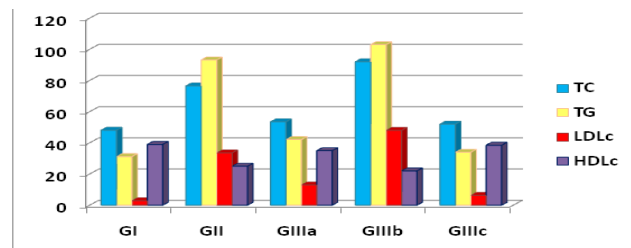
△ A significant increase compared with high fat diet group (GII) and ovariectomized rats fed on high fat diet (GIIIb)

○ A significant increase compared with control group (GI).

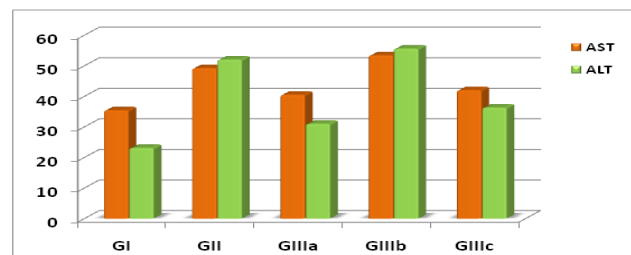
● A significant decrease compared with control group (GI).



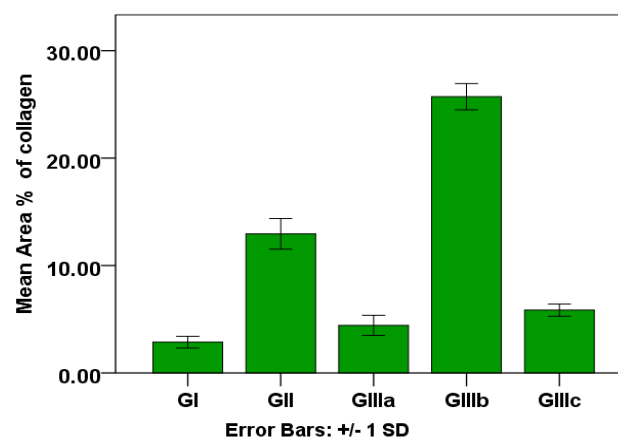
**Histogram 1:** The mean values of initial and final body weight (g) among all the experimental groups.



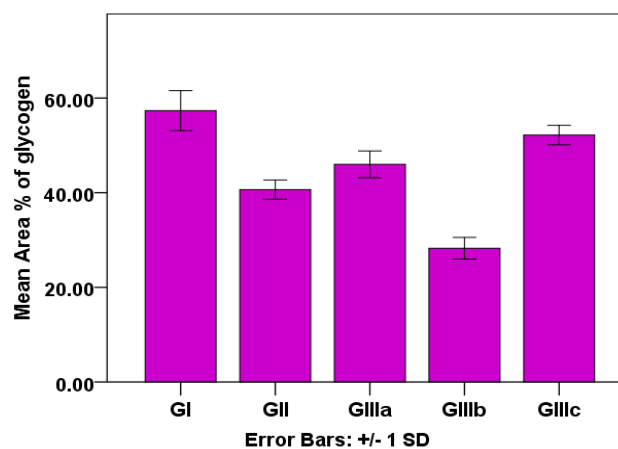
**Histogram 2:** The mean values of serum lipid profile (mg/dl) among all the experimental groups at the end of 12<sup>th</sup> week.



**Histogram 3:** The mean values of serum hepatic enzymes level (AST & ALT) (U/I) among all the experimental groups at the end of 12<sup>th</sup> week.



**Histogram 4:** The mean values of % of collagen area in liver tissue among all the experimental groups.



**Histogram 5:** The mean values of area % of glycogen in liver tissue among all the experimental groups.

## DISCUSSION

Postmenopausal obesity is generally the most part a significant danger for some ongoing illnesses as metabolic syndrome which is characterized by dyslipidemia, hypertension, insulin resistance, type II diabetes and cardiovascular problems that have been connected to the advancement of non-alcoholic fatty liver disease<sup>[1]</sup>.

These liver issues start as steatosis and may advance to steatohepatitis, cirrhosis, liver failure, and hepatocellular carcinoma<sup>[2]</sup>.

Since flaxseed and its items have pulled in a lot of interest among purchasers and medical services experts for their possible advantages on human wellbeing.

Since flaxseed and its products have attracted a great deal of interest among consumers and health care professionals for their potential benefits on human health<sup>[13]</sup>, so this study attempted to explain its impact on decreasing body, improving lipid profile, hepatic enzymes levels and enhancing the histological changes on the liver of ovariectomized adult female albino rat fed on fat-enriched diet.

Ovariectomy of an adult female albino rat was performed to make these animals in a physiological condition simulating menopause<sup>[25]</sup> then an obese rat model based on a high-fat chow diet was developed to induce most of the pathogenic findings in the nonalcoholic fatty liver disease (NAFLD) such as hepatic steatosis, oxidative stress, necroinflammatory liver injury and collagen deposition in obese postmenopausal women<sup>[26]</sup>.

Crushed flaxseed at a dose of 0.2 gm/day/rat corresponded to the adult human dose of 50 gm/day that was reported according to the study of Cunnane *et al.*<sup>[16]</sup> to cause a significant reduction in the serum lipid profile.

The body-weight increase was a well-documented observation in the ovariectomized rat fed on a balanced diet (GIIIa) and the high-fat diet groups (GII, GIIIb) which be related to the occurrence of leptin resistance across the central nervous system as a consequence of withdrawal of ovarian hormones that end to accelerate fat deposition and increment weight to hoist coursing endogenous estrogens from peripheral aromatization of androgens in adipose tissue followed by diminishes motor activity in obese postmenopausal women<sup>[27]</sup>.

An increase in the serum lipid parameters; TC, TG, LDLc levels coupled with a significant decrease in HDLc that were detected in the ovariectomized (GIIIa) and the high-fat diet groups (GII & GIIIb) when compared to those of the control was in agreement with Sarrel *et al.*<sup>[28]</sup> who expressed that reformist withdrawal of estrogen during natural menopause or following bilateral ovariectomy is associated with decays of the blood lipid profile just as numerous highlights of the metabolic syndrome.

Al-Awadi *et al.*<sup>[29]</sup> and Titchenell *et al.*<sup>[30]</sup> explained disturbance in lipid profiles by overfeeding and peripheral

insulin resistance with the excess in both blood glucose and free fatty acid (FFA) and subsequently increased the uptake of hepatic glucose that diverted into the hepatic de novo lipogenesis thus adds to expanding intra hepatocellular pool of FFA.

The elevation in hepatic enzymes (AST& ALT) that were recorded in GII and GIIIb were in concurrence with Ingawale *et al.*<sup>[31]</sup> who stated that ALT and AST are the most specific intracellular enzymes that are associated with cell leakage and serve as a marker of hepatocellular injury with greater grades of hepatic steatosis and fibrosis in population studies. They attributed this elevation to an increase in the production of free radicals that initiate lipid peroxidation of membrane leading to loss of integrity of cell membranes and damage of hepatic cells.

Light microscopic studies were carried out on approximately the same area of the right lobe of the liver according to the study of Venkatesh<sup>[32]</sup> who stated that the right lobe shows more homogenous steatosis than the left lobe.

The hepatic histological findings in the current study went parallel with the serological results. The most prominent signs of liver deterioration in H&E stained sections in the ovariectomized (GIIIa) and the high-fat diet groups (GII & GIIIb) were in the form of multiple intracytoplasmic vacuoles described as microvesicular steatosis with extensive diffuse large intracytoplasmic vacuoles described by Sakamoto *et al.*<sup>[33]</sup> as macrovesicular steatosis with an irregular orientation of the hepatocyte plates. Moreover, there were congested central and portal veins, inflammatory cell infiltration and hemorrhagic areas within all zones of hepatic lobules.

Titchenell *et al.*<sup>[30]</sup> found that hepatic insulin resistance is the key pathogenic factor for the hepatocellular injury and the development of hepatic steatosis due to the direct cytotoxicity of the fatty acids on the hepatocytes as a result of excessive 'de novo' synthesis of fatty acids, impairs their metabolism and export from hepatocytes which lead to prominent intracellular triglycerides accumulation (fatty liver).

Oxidative stress and the formation of reactive oxygen species (ROS) is thought to be the main mechanism of the hepatocellular injury which in turn may induce lipid peroxidation, apoptosis dysregulation, mitochondrial cytopathies, a defective  $\beta$ -oxidation of fatty acids with high expression of proinflammatory cytokines and decreased levels of anti-inflammatory cytokines resulting in oxidative stress, that linked to the tissue parenchymal damage and cell death<sup>[34]</sup>.

Hassan *et al.*<sup>[35]</sup> attributed irregular orientation of the hepatocyte plates in GIIIb to the oxidative damage of hepatocellular proteins or necrotic changes in hepatocytes as a consequence of severe steatohepatitis.

The inflammatory cells infiltration detected in the current study might be due to the estrogen deficiency



following bilateral ovariectomy and the absence of its antioxidant effects in preventing macrophage accumulation, increasing the sensitivity of Kupffer cells to endotoxins and suppressing the spontaneous expression of pro-inflammatory mediators and multiple gene transcription factors such as activator protein-1 (AP-1) and nuclear transcription factor-Kappa-B (NF-κB)<sup>[36]</sup>.

In the present study, a significant increase in the density and distribution of collagen fibers mainly at the portal tract area in the ovariectomized (GIIIa) and the high-fat diet groups (GII & GIIIb) in Masson's trichrome-stained sections was most probably due to reactive oxygen species overproduction, apoptosis dysregulation, increase proinflammatory cytokines expressions and locally produced a fibrogenic growth factor such as platelet-derived growth factor (PDGF-β) and transforming growth factor (TGF-β) which directly increased the activity of hepatic stellate cells (HSCs) which in turn lost their lipid and vitamin A storage capability and differentiated into myofibroblast-like cells that is the major source of extracellular matrix secretion as well as increase the expression of tissue matrix metalloproteinase I and II with increase deposition of type I and type III collagen within the perisinusoidal space, ending up with progressive liver fibrosis<sup>[37,38]</sup>.

Chicken wire fibrosis that was observed in GIIIb was particularly attributed to the apparent vacuolated hepatocytes that pressing the collagen fibers from more than one side<sup>[38,39]</sup>.

A significant decrease in the area percentage of glycogen within the vacuolated hepatocytes on using the PAS technique that was observed in the high-fat diet groups (GII & GIIIb) could be attributed to the insulin resistance with excess utilization of hepatic glucose for hepatic de novo lipogenesis and the accumulation of triglycerides within hepatocytes, thus reduced glycogen stores in the fatty liver<sup>[29]</sup>. Defective activation of glycogen synthase enzyme which participating in liver glycogenesis is another theory stated by Titchenell *et al.*<sup>[30]</sup>.

However, Imtiaz *et al.*<sup>[40]</sup> stated in their studies that there is no demonstrable association between the fat content of the hepatocytes and the presence of hepatic glycogen.

Electron microscopic examination of the liver of the ovariectomized rats fed on a high-fat diet confirmed all findings depicted previously with numerous electron lucent lipid droplets coalesced with each other, degenerated giant swollen mitochondria, dilated rough endoplasmic reticulum, secondary lysosomes and areas of rarefied cytoplasm. Inflammatory cells were detected in the hepatic sinusoids. Moreover, lipid droplets are scattered in the hepatic sinusoids and the endothelial lining cells. Kupffer cells contained lysosomes and phagocytic vesicles were seen. Collagen bundles nearby flattened myofibroblast were also observed.

Studies by Forrester *et al.*<sup>[41]</sup> and Mansouri *et al.*<sup>[42]</sup> attributed macrovesicular steatosis and progressively

degenerated mitochondria to excess triglycerides synthesis, changes in hepatic enzymes and oxidative stress upregulated the proapoptotic genes. This trigger changing the mitochondrial inner membrane composition, translocation of intra-mitochondrial protein (apoptosis-inducing factor), enhancing the carnitine palmitoyl transferase (CPT-I) on the inner mitochondrial membrane which increases the entry of long-chain fatty acids into mitochondria, decreases in proton leak with subsequent damaging mitochondrial DNA directly with ATP depletion. Thus reducing mitochondrial respiratory capacities and increasing the activity of hepatic peroxisome proliferator-activated receptor-α ending with structural alterations of the mitochondrial matrix, mitochondrial swelling through the apoptotic pathway.

Yuzefovych *et al.*<sup>[43]</sup> attributed the dilated rough endoplasmic reticulum in the present study to fatty changes with increased synthesis of proteins that bound the excess free fatty acids to form lipoproteins and triglycerides which is catalyzed by triacylglycerol synthesizing enzymes at the rough endoplasmic reticulum.

The presence of multivesicular bodies (secondary lysosomes) seems to be an obligatory intermediate step in the degradation of lipoprotein remnants, the damaged portion of hepatocyte cytoplasm, necrotic debris and many other ligands<sup>[44]</sup>.

Kupffer cells exhibited excess lysosomal protease activity, and output of biologically active mediators functioning in phagocytosis in the HFD group<sup>[42,43]</sup>.

The rarefied cytoplasm which was observed in hepatocytes of (GIIIb) is likely a representation of cells undergoing lytic necrosis<sup>[42]</sup>.

Lipid droplets that were observed in the hepatic sinusoids of GIIIb may have been partially hydrolyzed, probably by lipoprotein lipase followed by crossing small-sized lipid particles the endothelial fenestrations to enter the spaces of Disse and are afterward internalized to some extent by hepatocytes but mainly by sinusoidal endothelial cells. However, the role of the nonparenchymal cells in the uptake and processing of lipoprotein remnants is controversial<sup>[45]</sup>.

Activated myofibroblast-like HSCs cells in the subendothelial space of Disse was in agreement with Senoo *et al.*<sup>[46]</sup> who attributed the occurrence of fibrosis in the fatty liver to the activation of hepatic stellate cells which response by changing its fine structure considerably such as dramatically losing their characteristic lipid droplets with the expansion of its rough endoplasmic reticulum accompanied with a well developed Golgi apparatus, as a result of active protein synthesis suggesting that hepatic stellate cells are the key cells in the hepatic fibrosis.

Flaxseed in the ovariectomized high-fat diet group (IIIc) revealed marked improvement in the body weight, serological and histological parameters of the liver, restoration of the hepatic architecture as compared to

the high-fat diet groups (II, IIIb). However, their levels couldn't reach normal levels.

The reduction in body weight was attributed to the lecithin content in freshly squashed flaxseed which breaks up the frightful fats from food in the digestive tract and eliminated them from the body. Likewise, water-soluble fibers and protein substances of flaxseed are slowly processed, postpone gastric purging and will in general increment intestinal transit time, give a sensation of fullness for a longer time and stifle craving<sup>[47]</sup>. Moreover, alpha-linolenic acid content increases the the body's affectability to the leptin hormone which lessens feeding behavior, stimulates thyroid function, speeds up metabolism and furthermore perhaps increments thermogenic activity in brown adipose tissue<sup>[39]</sup>.

The mechanism by which flaxseed reduces plasma lipids and improves hepatic steatosis is unclear and has not been fully identified. Elimam *et al.*<sup>[39]</sup> attributed the hypocholesterolemic effects of flaxseed to increasing bile acid excretion and hepatic metabolism in a way that augments low-density lipoprotein cholesterol removal by hepatocytes.

Also, Monk *et al.*<sup>[47]</sup> declared that the water-soluble fiber substance of flaxseed may interact with cholesterol in the intestinal lumen and is completely converted in the colon into short-chain unsaturated fats which could hinder liver cholesterol synthesis and increment the body clearance of low-density lipoprotein cholesterol.

The presence of alpha-linolenic acid and linoleic acid (omega 3 and omega 6 respectively) in a perfect balance in flaxseed work together to become prostaglandins and may play vital roles in decreasing leakage of free fatty acids from peripheral adipose tissue back to the liver and also stimulating hepatic mitochondrial  $\beta$ -oxidation which in turn, play a big role in controlling blood cholesterol<sup>[48]</sup>. Besides, Fukumitsu *et al.*<sup>[49]</sup> and Jangale *et al.*<sup>[50]</sup> stated that alpha-linolenic acids and lignans contents are potent activators of peroxisome proliferator-activated receptor- $\alpha$  (PPAR  $\alpha$ ) that is the potent suppressors of fatty acid and triacylglycerol synthesis and inducers of fatty acid oxidation.

The hepatoprotective effects of flaxseed with improving liver enzymes (AST & ALT) levels may be related to the effect of alpha-linolenic acids on the hepatocyte itself, the stability of hepatocytes cell membrane and the proper activity of the membrane-bound proteins thus maintaining its fluidity and produce flexible cell membranes<sup>[50]</sup>.

Marked improvement in the histological structure of the liver in GIIIc may be related to the hypolipidemic effect of alpha-linolenic acid, lignans and water-soluble fiber contents of flaxseed that are potent antioxidants and may play an important role in improving insulin resistance that helps to reduce inflammatory responses by about 30% in many chronic diseases, promoting the immune response and downregulation of proinflammatory mediators such

as TNF-  $\alpha$ , interferon- $\gamma$  (IFN- $\gamma$ ) and fibrogenic growth factors<sup>[50]</sup>. Also, Hendawi *et al.*<sup>[51]</sup> stated that phytoestrogens in lignans of ground flaxseed provide a hepatoprotective role by acting on hepatic estrogen receptors that were reported to be protective against hepatocytes injury.

The alpha-linolenic acid and lignans contents of flaxseed may have an uncertain role in activating liver enzyme glycogen synthase and phosphorylase throughout the liver acinus which participating in liver glycogenesis instead of being diverted into the hepatic de novo lipogenesis<sup>[50,51]</sup>.

## CONCLUSION

The present study has generated evidence that the absence of a normal estrogenic status in postmenopausal women constitutes a potential risk factor for the development of obesity, hyperlipidemia and synergistically favors fatty liver, especially when combined with feeding on a high-fat diet. Furthermore, dietary supplementation with crushed flaxseed markedly reduced body weight, hyperlipidemia, improved liver enzymes and is considered as a potent antioxidant agent having a hepatoprotective role against steatohepatitis and fibrosis in ovariectomized obese rat model. Although the mechanisms remain unclear they are most probably mediated by alpha-linolenic acid, fibers and phytoestrogens in lignans that have a chemical structure similar to that of endogenous estrogen.

## CONFLICT OF INTERESTS

There are no conflicts of interest.

## REFERENCES

1. Lindenmeyer CC and McCullough A J. The Natural History of Nonalcoholic Fatty Liver Disease - An Evolving View. *Clinical liver disease*. 2018; 22(1): 11–21.
2. Stefan N, Häring HU and Cusi K. Non-alcoholic fatty liver disease: Causes, diagnosis, cardiometabolic consequences, and treatment strategies. *Lancet Diabetes and Endocrinology*. 2018; 7 (4): 313-324.
3. Zou TT, Zhang C, Zhou YF, Han YJ, Xiong JJ, Wu XX, Chen YP and Zheng MH. Lifestyle interventions for patients with nonalcoholic fatty liver disease. *Eur. J. Gastroenterol. Hepatol*. 2018; 30: 747–755.
4. Nalbantoglu I and Brunt EM: Role of liver biopsy in nonalcoholic fatty liver disease. *World J Gastroenterol*. 2014; 20 (27): 9026-9037.
5. Abd El-Kader SM and Ashmawy ES: Non-alcoholic fatty liver disease: The diagnosis and management. *World J Hepatol* . 2015; 28; 7(6): 846-858.
6. Eslamparast T, Tandon P and Raman M. Dietary composition independent of weight loss in the management of non-alcoholic fatty liver disease. *Nutrients*. 2017; 9 (8):800-819.

7. Gepner Y, Shelef I, Komy O, Cohen N, Schwarzfuchs D, Brill N, Rein M, Serfaty D, Kenigsbuch S *et al.* The beneficial effects of Mediterranean diet over low-fat diet may be mediated by decreasing hepatic fat content. *J Hepatol.* 2019; 71(2):379–388.
8. Friedman SL, Neuschwander-Tetri B.A., Rinella M. and Sanyal A.J. Mechanisms of NAFLD development and therapeutic strategies. *Nat. Med.* 2018; 24 (7): 908–922.
9. Verbeek J, Spincemaille P, Vanhorebeek I, Van den Berghe G, Vander Elst I, Windmolders P, van Pelt J, van der Merwe S, Bedossa P, Nevens F *et al.* Dietary intervention, but not losartan, completely reverses non-alcoholic steatohepatitis in obese and insulin resistant mice. *Lipids Health Dis.* 2017; 16 (46): 1–10.
10. Farhan AR. Evaluation of Melatonin Hormone and Nitric oxide Levels in Non-alcoholic Fatty Liver Patients in Relation to Obesity and Oxidative Stress. *J. Pharm. Sci. Res.* 2018; 10 (5):1167–1169.
11. Tokodai K, Karadagi A, Kjaermet F, Romano A, Ericzon B and Nowak G. Characteristics and risk factors for recurrence of nonalcoholic steatohepatitis following liver transplantation. *Scand J Gastroenterol.* 2019; 54 (2):233-239.
12. Jamshidi-Kia F, Lorigooini Z and Amini-Khoei H. Medicinal plants: Past history and future perspective. *Journal of Herbmec Pharmacology.* 2018; 7(1): 1-7.
13. Parikh M, Netticadan T and Pierce GN. Flaxseed: Its bioactive components and their cardiovascular benefits. *Am. J. Physiol. Heart Circ. Physiol.* 2018; 314 (2): H146–H159.
14. Calvert CS, Benevenga NJ, Eckhart CD, Fahey GC, Greger JL, Keen CL, Knapka JJ, Magalhaes H and Oftedal OT. Nutrient requirements of the laboratory rat. In: *Nutrient Requirements of Laboratory Animals*, 4th edition, Chapter 2. National Academy Press, Washington, D.C.1995; 11-79.
15. Buettner R, Parhofer KG, Woenckhaus M, Wrede CE, Kunz-Schughart LA, Schölmerich J and Bollheimer LC. Defining high fat-diet rat models: metabolic and molecular effects of different fat types. *Journal of Molecular Endocrinology.* 2006; 36(3): 485-501.
16. Cunnane SC, Ganguli S, Menard C, Liede AC, Hamadeh MJ, Chen ZY and Wolever TM. High alpha linolenic acid flaxseed (*Linum usitatissimum*): some nutritional properties in humans. *Br J Nutr.* 2006; 69 (2):443-453.
17. Liu XL, Li CL, Lu WW, Cai WX and Zheng LW. “Skeletal site-specific response to ovariectomy in a rat model: change in bone density and microarchitecture,” *Clinical Oral Implants Research.* 2015; 26 (4):392–398.
18. Abdel – Rahman MK, Mahmoud EM, Abdel-Moemin AR and Rafaat OG. Re-evaluation of individual and combined garlic and flaxseed diets on hyperlipidemic rats. *Pakistan Journal of Nutrition.* 2009; 8 (1): 1-8.
19. Merghani BH, Awadin WF, Elseady YY and Abu-Heakal NSA. Protective Role of Wheat Germ Oil against Hyperglycemia and Hyperlipidemia in Streptozotocin Induced Diabetic Rats. *Asian Journal of Animal and Veterinary Advances.* 2015; 10 (12): 852-864.
20. Penumarthy S, Penmetsa GS and Mannem S. Assessment of serum levels of triglycerides, total cholesterol, high-density lipoprotein cholesterol, and low-density lipoprotein cholesterol in periodontitis patients. *J Indian Soc Periodontol.* 2013; 17(1): 30–35.
21. Bancroft JD and Layton C. The hematoxylin and eosin, connective mesenchymal tissues with their stains In: Suvarna SK, Layton C and Bancroft JD (eds). *Bancroft’s Theory and practice of histological techniques.* (7th edition). Churchill Livingstone, Philadelphia. 2013; pp 173-212 and 215-238.
22. Woods AE and Stirling JW. Transmission electron microscopy. *Bancroft’s theory and practice of histological techniques.* 8th edition, Churchill Livingstone, Elsevier, China. 2018; pp.434-475.
23. El Morsey DM, Abou-Rabia NM., Khalaf G and Ezzat SF. Histological Study on the Possible Protective Role of Moringa Oleifera Leaves Extract on Paracetamol Induced Liver Damage in Adult Male Albino Rats. *EJH.* 2019; 42(3):712-729.
24. McHugh ML. Multiple comparison analysis testing in ANOVA. *Biochemia Medica.* 2011; 21(3):203-209.
25. Panneerselvam S, Packirisamy RM, Bobby Z and Sridhar MG. Protective effect of soy isoflavones (from *Glycine max*) on adipose tissue oxidative stress and inflammatory response in an experimental model of post-menopausal obesity: The molecular mechanisms. *Biochem Anal Biochem.* 2016; 5(2): 266-273.
26. Ipsen, DH, Lykkesfeldt J and Tveden-Nyborg P. Molecular mechanisms of hepatic lipid accumulation in non-alcoholic fatty liver disease. *Cell Mol. Life Sci.* 2018; 75(18): 3313–3327.
27. Mauvais-Jarvis F, Clegg DJ and Hevener AL. The Role of Estrogens in Control of Energy Balance and Glucose Homeostasis. *Endocr Rev.* 2013; 34(3): 309–338.
28. Sarrel PM, Sullivan SD and Nelson LM. Hormone replacement therapy in young women with surgical primary ovarian insufficiency. *Fertil Steril.* 2016; 106 (7):1580–1587.

29. Al-Awadi JH, Rashid KH and Hassen AJ. High fat diet induce hyperlipidemia incidences with sever changes in liver tissue of male albino rats: A histological and biochemical Study. *Kerbala J Pharm Sci.* 2013; 6 (1):21–32.
  30. Titchenell PM, Quinn WJ, Lu M, Chu Q, Lu W, Li C, Chen H, Monks BR, Chen J, Rabinowitz JD and Birnbaum MJ. Direct Hepatocyte Insulin Signaling Is Required for Lipogenesis but Is Dispensable for the Suppression of Glucose Production. *Cell Metab.* 2016; 23 (6):1154–1166.
  31. Ingawale DK, Mandlik SK and Naik SR. “Models of hepatotoxicity and the underlying cellular, biochemical and immunological mechanism(s): a critical discussion,” *Environmental Toxicology and Pharmacology.* 2014; 37(1): 118–133.
  32. Venkatesh SK. Liver Masses: A Clinical, Radiological and Pathological Perspective For: Perspectives in Clinical Gastroenterology and Hepatology *Clin Gastroenterol Hepatol .* 2014; 12(9): 1414–1429.
  33. Sakamoto M, Tsujikawa H, Effendi K, Ojima H, Harada K, Zen Y, Kondo F, Nakano M, Kage M, Sumida Y, Hashimoto E, Yamada G, Okanoue T and Koike K. “Pathological findings of nonalcoholic steatohepatitis and nonalcoholic fatty liver disease,” *Pathology International.*2017; 67 (1): 1–7.
  34. Jung ES, Lee K, Yu E, Kang YK, Cho M-Y, Kim JM, Moon WS, Jeong JS, Park CK, Park J-B, Kang DY, Sohn JH and Jin S-Y. Interobserver Agreement on Pathologic Features of Liver Biopsy Tissue in Patients with Nonalcoholic Fatty Liver Disease *.Journal of Pathology and Translational Medicine.* 2016; 50(3): 190-196.
  35. Hassan NF, Soliman GM, Okasha EF and Shalaby AM. Histological, Immunohistochemical, and Biochemical Study of Experimentally Induced Fatty Liver in Adult Male Albino Rat and the Possible Protective Role of Pomegranate. *J Microsc Ultrastruct.* 2018; 6(1): 44–55.
  36. Tan Y, Lao W, Xiao L, Wang Z, Xiao W, Kamal MA, Seale JP and Qu X. Managing the combination of nonalcoholic fatty liver disease and metabolic syndrome with Chinese herbal extracts in high-fat-diet fed rats. *Evid Based Complement Alternat Med.* 2013; 2013: 306738.
  37. Xie G, Wang X, Wang L, Wang L, Atkinson RD, Kanel GC, Gaarde WA and Deleve LD. Role of differentiation of liver sinusoidal endothelial cells in progression and regression of hepatic fibrosis in rats. *Gastroenterology.* 2012; 142(4):918–927.
  38. Kim MY. “The Progression of Liver Fibrosis in Non-alcoholic Fatty Liver Disease,” *The Korean Journal of Gastroenterology.* 2017; 69 (6): 341–347.
  39. Elimam H and Ramadan BK . Comparative Study of the Possible Prophylactic and Curative Effects of Flaxseed Oil on the Lipid Profile and Antioxidant Status of Hyperlipidaemic Rats. *J Appl Pharm.* 2018; 10 (1): 257-263.
  40. Imtiaz KE, Healy C, Sharif S, Drake I, Awan F, Riley J and Karlson F. Glycogenic hepatopathy in type 1 diabetes: an underrecognized condition. *Diabetes Care.* 2013; 36 (1):e6–e7.
  41. Forrester J, Kikuchi DS, Hernandez MS, Xu Q and Griendling KK. Reactiveoxygen species in metabolic and inflammatory signaling, *Circ. Res.* 2018; 122 (6): 877–902.
  42. Mansouri A, Gattolliat C-H and Asselah T. Mitochondrial dysfunction and signalingin chronic liver diseases, *Gastroenterology.* 2018; 155 (3): 629–647.
  43. Yuzefovych L V, Musiyenko SI, Wilson GL, and Rachek L I. Mitochondrial DNA damage and dysfunction, and oxidative stress are associated with endoplasmic reticulum stress, protein degradation and apoptosis in high fat diet-induced insulin resistance mice. *PLoS one.* 2013; 8 (1): e54059.
  44. Skop V, Cahova M, Papackova Z, Palenickova E, Dankova H, Baranowski M, Zabielski P, Zdychova J, Zidkova J, and Kazdova L. Autophagy-lysosomal pathway is involved in lipid degradation in rat liver. *Physiol Res.* 2012; 61(3): 287-297.
  45. Cogger VC , Roessner U, Warren A, Fraser R, David G and Couteur L. A Sieve-Raft Hypothesis for the regulation of endothelial fenestrations. *Comput Struct Biotechnol J.*2013; 8(11): e201308003.
  46. Senoo H, Mezaki Y and Fujiwara M. The stellate cell system (vitamin A-storing cell system). *Anatomical Science International journal.* 2017; 92: 387–455.
  47. Monk JM, Liddle DM, Brown MJ, Zarepoor L, De Boer AA, Ma DWL, Power KA and Robinson LE. “Anti-inflammatory and anti-chemotactic effects of dietary flaxseed oil on CD8+ T cell/adipocyte-mediated cross-talk,” *Molecular Nutrition & Food Research.*2016; 60(3): 621–630.
  48. Toure A and Xueming X. Flaxseed lignans: source, biosynthesis, metabolism, antioxidant activity, bio-active components and health benefits. *Compr Rev Food Sci Food Saf.* 2010; 9:261–269.
  49. Fukumitsu S, Aida K, Shimizu H and Toyoda K: Flaxseed lignan lowers blood cholesterol and decreases liver disease risk factors in moderately hypercholesterolemic men. *Nutr Res.* 2010; 30(7):441-6.
-

50. Jangale NM, Devarshi PP, Bansode SB, Kulkarni MJ and Harsulkar AM. "Dietary flaxseed oil and fish oil ameliorates renal oxidative stress, protein glycation, and inflammation in streptozotocin-nicotinamide-induced diabetic rats" *Journal of Physiology and Biochemistry*.2016; 72(2): 327–336.
51. Hendawi MY, Alam RT, and Abdellatief SA. "Ameliorative effect of flaxseed oil against thiacloprid-induced toxicity in rats: hematological, biochemical, and histopathological study," *Environmental Science and Pollution Research International*. 2016; 23(12): 11855–11863.

## الملخص العربي

# تأثير الغذاء عالي الدهون وبذور الكتان على التركيب النسيجي والتركيب الهستوكيميائي والقياسات النسيجية لكبد الجرذ الابيض المستأصل المبايض

حكمت احمد سرور، منى عبد الرحمن سالم، دينا علام عبد المقصود، منى محمد عبد الجليل

قسم الهستولوجيا - كلية الطب (بنات) - جامعة الازهر

**مقدمة البحث:** تعد زيادة الوزن بعد انقطاع الطمث إنذاراً لصحة المرأة حيث أنها قد تؤدي إلى مرض الكبد الدهني غير الكحولي. وتمتاز بذور الكتان بأنها غنية بمضادات الأكسدة مما قد يحسن من وظائف الكبد. وبالرغم من ذلك، لا تزال الآليات الدقيقة غير واضحة.

**الهدف:** تهدف هذه الدراسة الى تقييم الدور الوقائي لبذور الكتان على نسيج الكبد في الجرذان البيضاء المستأصلة المبايض.

**المواد والطرق:** تم تقسيم إناث الجرذان البيضاء البالغة إلى ثلاث مجموعات: المجموعة الأولى (المجموعة الضابطة)، المجموعة الثانية (مجموعة النظام الغذائي عالي الدهون) والمجموعة الثالثة (المجموعة المستأصلة المبايض) التي تم استئصال المبايض منها ثم قسمت تلك المجموعة بالتساوي إلى GIIIa (مجموعة مستأصلة المبايض فقط)، GIIIb (جرذان مستأصلة المبايض وتغذت على نظام غذائي عالي الدهون) و GIIIc (جرذان مستأصلة المبايض وتغذت على نظام غذائي عالي الدهون يحتوي على مسحوق بذور الكتان) حتى نهاية التجربة. بعد ١٢ أسبوعاً تم تقدير وزن الجسم وقياس مستويات الدهون في الدم وإنزيمات الكبد. ثم تم تحضير عينات الكبد لفحصها نسيجياً بالميكروسكوب الضوئي والالكتروني. كما أجريت القياسات المورفومترية والتحليلات الإحصائية.

**النتائج:** تسبب استئصال المبايض والنظام الغذائي عالي الدهون في زيادة كبيرة في وزن الجسم، ومستويات الدهون بالدم، وحدوث تغيرات مدمرة في أنسجة الكبد على هيئة فجوات بالسيتوبلازم، وانوية ضامرة مع احتقان الشعيرات الدموية البينية وتسلل الخلايا الالتهابية التي اقترنت بارتفاع أنزيمات الكبد مصحوباً بارتفاع كبير في النسبة المئوية من مساحة ألياف الكولاجين وانخفاض ملحوظ في تفاعل (PAS). وقد أكد التركيب النسيجي الدقيق هذه التغيرات. بينما أظهرت المجموعة المعالجة بمسحوق بذور الكتان تحسناً ملحوظاً في مستويات دهون الدم والمعايير الكيميائية الحيوية لوظائف الكبد مع تحسناً كبيراً في التغيرات النسيجية للكبد الموضحة سابقاً.

**الخلاصة:** قد يكون لبذور الكتان دور وقائي ضد التهاب الكبد الدهني وتليف الكبد في نموذج الجرذان البيضاء المستأصلة المبايض.